Proceeding of the IEEE
International Conference on Robotics and Biomimetics
Dali, China, December 2019

Super-Resolution reconstruction of Bone Micro-Structure Micro-CT Image based on Auto-Encoder Structure*

Xuyang Xie[1,2], Yu Wang[1,3], Shibo Li[1]*, Long Lei[1], Ying Hu[1]*, Jianwei Zhang[4]
1 *Shenzhen Key Laboratory of Minimally Invasive Surgical Robotics and System, Shenzhen Institutes of Advanced Technology, Chinese Academy of Sciences*
2 *University of Chinese Academy of Sciences*
3 *Harbin Institute of Technology, Shenzhen*
4 TAMS, Department of Informatics, University of Hamburg, Hamburg, Germany
**Correspondence: sb.li@siat.ac.cn (Shibo Li), ying.hu@siat.ac.cn (Ying Hu).*

***A*bstract—Computed Tomography (CT) is widely used for screening, diagnostic and image-guided therapy for clinical and research purposes. The current Finite Element Analysis for Research Microstructure based on Micro-CT scan data has been considered the gold standard for non-invasive studies of bone microstructure. In medical diagnosis and treatment, the resolution of clinical medical images is low, and it is impossible to directly observe the fine structure of bone through Micro-CT. However, there are many problems in high resolution image, such as long scan time, high radiation dose and complicated processing steps. Therefore, the research goal of this paper is to propose a new network structure which can reconstruct high-resolution bone microstructure images with fine structure while reducing X-ray radiation. The network model proposed in this paper combines the auto-encoder structure and adopts a staged up-sampling strategy to accurately reconstruct high-resolution images from low-resolution images.**

Moreover, in order to be more realistic, this paper constructs a real training data set according to strict operation. In the data set of this paper, a variety of existing super-resolution reconstruction methods are used for comparison test. The results show that the network model proposed in this paper achieves better reconstruction results. We found in the experiment that the noise of the sample itself has a certain influence on the evaluation of the reconstruction effect and the impact of noise reduction is also discussed on super-resolution reconstruction.

Index Terms – auto-encoder, microstructure, Micro-CT image, super-resolution reconstruction

I. Introduction

Histological studies [1-3] have shown that bone micro-structure is an important determinant of bone strength and fracture risk. Clinical CT images cannot be refined for bone microstructure due to their low resolution, and are not suitable for clinical use of bone micro-structure-related diseases screening, diagnosis and treatment. Micro-CT has a high spatial resolution and allows quantitative analysis of bone microstructure, which has been widely used in clinical medicine. However, state-of-the-art CT imaging techniques only allow spatial resolution to be comparable or slightly higher than human trabecular bone thickness [4], making the micro-structure of a single trabecular bone relatively fuzzy, and its partial volume effect is significant, which increases the significant error in measurement and interpretation. Micro-CT has longer scanning time and larger ionizing radiation than clinical CT. Therefore, if the scanning time and ionizing radiation can be reduced, high-resolution images satisfying the fine structure requirements can be obtained, which will be very helpful for improving the accuracy and efficiency of related clinical applications and researches.

Image Super Resolution (SR) refers to the use of relevant knowledge in the fields of image processing, computer vision, etc., to reconstruct a corresponding high resolution from a given low resolution image (Low Resolution, LR) by a specific algorithm and processing flow. High Resolution (HR) image technology has a significant role in noise reduction and image resolution. Super-resolution reconstruction of medical images can reduce the requirements of the imaging environment without increasing the cost of high-resolution imaging technology, and achieve a fine display of fine structures through reconstructed high-resolution medical images to help doctors make a better diagnosis of the patient's condition.

According to different principles, image super-resolution methods can be divided into three categories: interpolation-based methods, model-based methods and learning-based methods. Interpolation-based Bicubic interpolation methods have high computational efficiency, but are easy to lose high frequencies texture detail. Model-based methods, such as using the a priori information to constrain the maximum posterior probability (MAP) method of the solution space [5]. Compared with the interpolation-based method, the performance of the method is improved. However, when the size of the input image is small, a priori information that can be effectively utilized is less, resulting in poor performance.

The learning-based approach can be divided into a compression-based [6] method and a deep-learning-based [7] method. Compressed sensing is a technique for efficiently acquiring and reconstructing signals by finding solutions to underdetermined linear systems. This is based on the principle that by optimization, signal sparsity can be used to recover signals from samples that are much less demanding than the Nyquist-Shannon sampling theorem. Sparse representation-based methods can preserve edge texture better, but compared with interpolation-based and model-based methods, it is difficult to learn higher-level abstract features, and when the super-resolution scaling is large, these methods also cannot achieve. Since Dong Chao et al. [8] obtained a better super-resolution reconstruction effect using the SRCNN network

*This research is supported by the National Natural Science Foundation of China (No. U1613224 and U1713218), the Key Fundamental Research Program of Shenzhen (No. JCYJ20180507182215361 and No. JCYJ20180507182415428) and Shenzhen Key Laboratory Project (Grant No. ZDSYS201707271637577)

model in 2016, the deep learning-based super-resolution reconstruction method has been popularized in the field of image enhancement (for example, noise reduction and Super resolution) shows higher performance. Chenyu You et al. [9] used a semi-supervised method to reduce the LR image by using a generated confrontation network (GAN) to effectively improve its resolution. And Hristina Uzunova et al. [10] used the generated antagonistic network for multi-scale stitching to generate large-size 2D and 3D high-resolution images, which provided a new idea for the application of large-size medical images, especially the SR reconstruction of 3D images. Antagonistic learning can learn feature representations in complex data distributions with significant success. However, in the field of super-resolution reconstruction, more attention is paid to improving the visual effect of images, but it does not ensure the consistency and integrity of the reconstructed images in structure and content. There is no doubt that it needs to be treated with caution for medical images.

For the traditional convolutional network, the presentation and application of the residual network bring significant benefits to the super-resolution reconstruction based on deep learning. It can not only improve the performance of the network model, but also pass the low-level information to the upper layer through the skip connection, making up for the loss of low-frequency information in the deep network. Chaudhari et al. [11] applied the residual network to super-resolution reconstruction and developed a CNN-based network for learning residual conversion from LR images to corresponding HR images. Yu et al. [12] proposed two advanced models based on CNN, which promote high-frequency texture by skipping the connection, and then fuse the high-frequency texture with the up-sampled image to generate an SR image. Therefore, the method in this paper also uses the residual network structure to reconstruct the high-resolution image with rich high-frequency details by using the low-frequency information of the LR image.

For super-resolution reconstruction of images, up-sampling magnification selection and steps are one of the more critical issues. From the super-resolution reconstruction study in the field of natural images, it can be found that the effect of SR reconstruction is decreasing as the up-sampling rate increases. Therefore, different up-sampling ratios will have different effects on SR reconstruction. Jia Liu et al. [13] focused on the problem of excessive up-sampling during super-resolution reconstruction, and proposed an edge-enhanced super-resolution confrontation network. The network proposes a two-stage super-resolution generation confrontation network for the problem of large sampling rate in single-direction MRI resolution, and uses the edge enhancement loss function to perform super-resolution reconstruction to provide more image details. The work in this paper is to perform 4 times up-sampling rate SR reconstruction on lower resolution Micro-CT images. In order to reduce the impact of high sampling rate, the second-order reconstruction strategy proposed by Lai W et al. [14] is used. Up-sampling is performed in stages, and different loss errors are given according to the reconstruction effects of the respective stages, thereby assisting the neural network to learn a more reliable feature representation.

In addition, Pan Liu et al. [15] proposed a new loss function based on real-order derivatives for small-scale reconstruction problems. This function can capture global image features, which performs well in high-frequency detail reconstruction. Kai Xuan et al. [16] injected the anisotropy of magnetic resonance imaging and integrated the input of multiple anisotropic image images, and proposed a super-resolution framework based on 3D depth learning to reconstruct isotropic high-resolution MR. image. Chen et al. [17] proposed a super-resolution network with deep dense connections, which transmits low-level information backwards layer by layer, and reconstructs high-resolution brain magnetic resonance (MR) images through rich information transmission.

The applications of deep convolutional networks, especially the residual network, densely connected networks and even the generation of confrontation networks, have brought new enhancements and expansions to SR reconstruction. However, the central issue of restoring finer texture details in images remains to be explored. The objective functions used in most networks are mainly focused on minimizing the mean squared reconstruction error, which can help the network model to obtain a higher peak signal-to-noise ratio, but less attention to structural similarity, which is still lacking for bone micro-structure and other clinically refined clinical diagnosis and treatment. The powerful feature extraction and expression capabilities of the auto-encoder can better help the network reconstruct more realistic and effective high-frequency details. In this paper, the super-resolution reconstruction of the Micro-CT image of the bone microstructure is proposed. A network model based on the auto-encoder structure is proposed. When the super-resolution reconstruction index is taken into consideration, more accurate and effective structural details can be obtained. The application and promotion of microstructure and Micro-CT in clinical application provides a way of thinking and direction.

In addition, Jinjin Gu et al. [18] found that most of the LR images used in super-resolution image reconstruction methods were obtained by HR images through interpolation and reduction sampling, which made the study of SR network model to a large extent the inverse of reduction sampling method. This will greatly affect the application of the SR model in the actual scenario. Therefore, for the SR reconstruction of bone microstructure, this paper does not use the mathematical method as in many previous studies to down-sample the HR image to obtain the LR image, but to construct the bone structure for the same part through strict scan setting. The actual super-resolution data set is fit, and a variety of existing network models are used for comparison verification to ensure the authenticity and effectiveness of the training data set.

This article will introduce the related work and results in more detail from the following aspects:

(1) The Method section will focus on the network structure and its details proposed in this paper;

(2) The Experiment section first introduces the construction of the data set in this paper, and then the relevant details of the network training. Finally, on the data set of this

paper, use a variety of network models to test and compare, and analyze the differences between them;

(3) The Discussion and Conclusion sections are based on the exploration and analysis of the problems in the experimental process, then summarize and plan the future exploration direction.

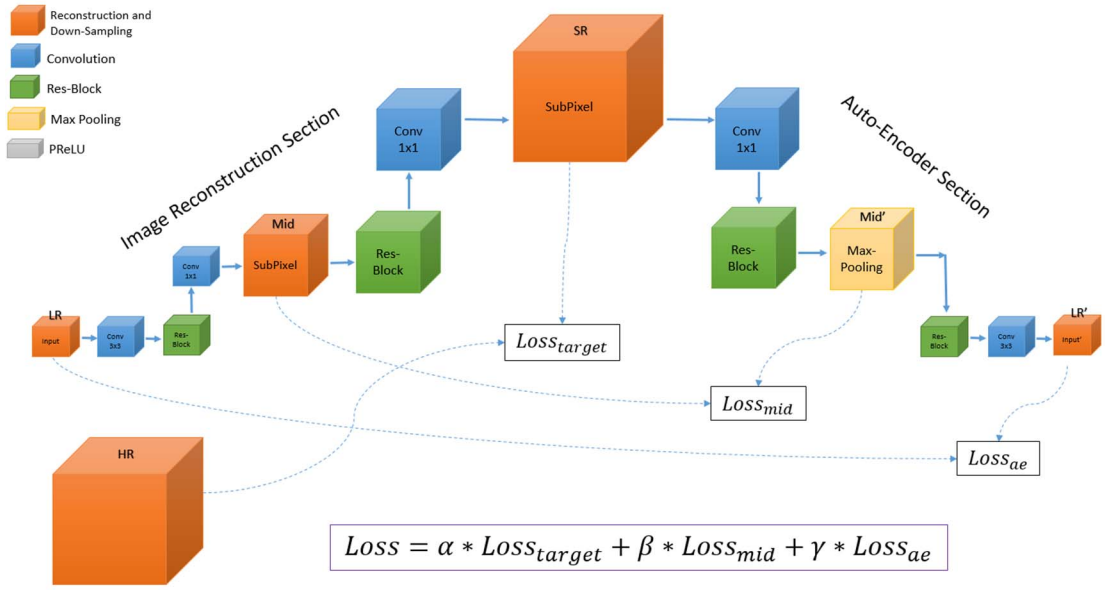

Figure 1 (a) AESR Network Structure

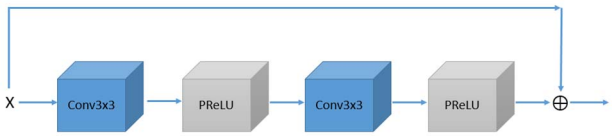

Figure 1 (b) Res-Block Structure

II. METHOD

A. Network Structure

The neural network model based on the auto-encoder structure proposed in this paper is shown in Figure 1(a) (called AESR), where LR represents the input low-resolution image and the input size is $W*H*C_1$, the input image is a grayscale image, i.e. C_1=1. HR represents a true high-resolution image. Different from the traditional auto-encoder inverted triangle structure, the whole network model presents a positive triangle structure through the convolution parameters. The setting ensures that the image size will not be reduced. For up-sampling, the sub-pixel method in Shi W et al. [19] is adopted. The core idea is neighborhood correlation, that is, by means of a convolutional network, extracting as many features of an LR image in a certain area. Then, by combining the features, the images are spliced into larger and higher resolution images. This allows for the reconstruction of details closer to the high-resolution image by screening and contrasting between the various combinations of groups.

For the image reconstruction part, the input image is first convolved by 3*3 kernel to generate $C_2 = 64$ feature maps. They will be sent to the Res-Block module shown in Figure 1 (b) for residual learning. Then a 1*1 convolution is added to generate $(\frac{scale}{2})^2 * C_2$ feature maps. Because the resolution of LR and HR is 4 (i.e. scale=4) times different in this paper, the sampling is performed in two stages, so the up-sampling ratio of each stage is 2. Then use the sub-pixel method to perform a 2x up-sampling of the first stage (denoted as Mid, size is $2W*2H*C_2$). The next 2x up-sampling of phase 2 is similar to the first phase. The image after two-stage up-sampling is called SR and the size is $4W*4H*C_3$. Then the Root Mean Square Error (RMSE) is used to assess the difference between HR and SR, recorded as $Loss_{target}$.

After the task of the reconstruction part is completed, it enters the auto-encoder section. Firstly, the SR is subjected to 1x1 convolution to generate SR', and then the feature extraction is performed by the Res-block module, and a 1*1 convolution is performed to perform 2 times down-sampling of the first stage to generate Mid'. Then the RMSE is calculated between the Mid' and Mid, recorded as $Loss_{mid}$. The second stage down-sampling process will generate LR' of the same size as the input image, the RMSE between them is recorded as $Loss_{ae}$.

In this way, the model training is guided by the weight of above three losses, so that the model can focus more on the

relationship between LR and HR in the process of learning, and reconstruct better high-resolution results.

B. Loss Function

The loss function in this paper is weighted by $Loss_{target}$, $Loss_{mid}$ and $Loss_{ae}$, whose expression is as follows:

$$Loss = \alpha * Loss_{target} + \beta * Loss_{mid} + \gamma * Loss_{ae} \quad (1)$$

The basic form of the loss function is the root mean square error (RMSE, as Eq.2).

$$L_2 = \sqrt{\frac{1}{N*W*H*C}\sum_{n}^{N}\sum_{i}^{W}\sum_{i}^{H}\sum_{c}^{C}(I^{HR}_{n,i,j,c} - I^{SR}_{n,i,j,c})^2} \quad (2)$$

where N, W, H, and C respectively represent the number of training samples, the image width and height, and the number of feature maps during the training. I^{HR}represents the ground truth HR image,I^{SR} represents the reconstructed image by the network model, as for $I_{n,i,j,c}$, it indicates the pixel value (the size is between 0 and 255) at the position of (i, j) in the c-th feature map of the n-th training sample. Based on model training results, the parameters are determined finally as $\alpha = 3$, $\beta = 1$, $\gamma = 2$。

III. Experiment

A. Dataset

The data set used in this paper is from real porcine bone scan data and the scanning device uses SCANCO MEDICAL AG in Switzerland. The scanning device generates low radiation during operation and does not cause harm to the human body. The scanning device model is μCT/100. The specific configuration is X-ray tube current 160μA, tube voltage 30-90kVp/20-50keV; resolution rated 1.25μm, 4μm (10%MTF@sample diameter 10mm), image matrix 512*512 To 8192*8192; detector 3702*400, photosensitive unit size 48μm; scanning size 100*140 mm (Ø*L).

The experimental scan sample was the end of the pig femur, and the Micro-CT scan was performed with a resolution of 30μm, (High Resolution) and 120μm, (Low Resolution) respectively. The scan sizes were 3000*3000 pixels and 750*750 pixels, respectively, and 1800 and 450 scanned images were obtained respectively.

According to the resolution multiple relationship of the two images, according to the image scanning serial number with a resolution of 30μm, one of the four images is extracted as HR, and a total of 450 images can be extracted, and 450 images with a resolution of 120μm, constitute a training sample pair. Then, on each pair of LR-HR sample pairs, three random crops were performed according to the scale, and the crop sizes were 125*125 pixels and 500*500 pixels respectively. The 861 pairs of LR-HR samples with better image structure were selected as training samples, 7 pairs of LR-HR sample pairs were used for testing.

B. Training Details

In the model training process, in order to retain more image information, the activation function adopts parameter ReLU, and the Batch Normalization layer is removed. The optimization method adopts Adam optimizer, and the initial learning rate is set to 5*1e-4, and according to the training process, attenuation of 0.9 per 10 epochs, training a total of 160 epochs.

In order to increase the contrast, in the training set constructed in this paper, Bicubic, SRCNN, FSRCNN[20], VDSR[21], EDSR[22], SRGAN[23] and LapSRN were selected for training, and the same test set was used for comparison. Based on the above-mentioned network structure, this paper extracts the trough and combines the feature expression ability of auto-encoder, and proposes a network model of AESR. Next, it will pass the two standard evaluation indicators of super-resolution PSNR (Peak Signal-to-Noise Ratio) and SSIM (Structural Similarity Index) to verify the feasibility of the proposed scheme. Among them, the values of PSNR and SSIM are as large as possible.

C. Results

The number of the test data set in this paper is based on the doctor's clinical experience, according to the order of the complexity of the bone microstructure in the Micro-CT image from high to low. The curve change in Figure 2(a) below shows the comparison of the PSNR of the evaluation indicators of different models on the same data set.

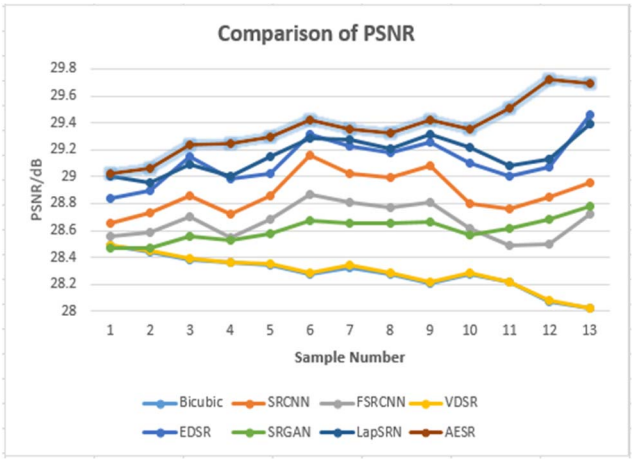

Figure 2(a) Comparison of test results of each model on the evaluation index PSNR

It can be seen from the PSNR curve that the AESR model proposed in this paper is always higher than other schemes, which proves the validity of the AESR model. It can also be found that the VDSR method based on deep learning has almost the same trend as the traditional interpolation Bicubic, and their performance is worse than that of other deep learning models. To analyze the reasons, the VDSR method is to deepen the level of the residual network and mix the images of different size multiples to support high-resolution reconstruction with different multiples. This method ignores the effects of different multi-resolution reconstructions, which is equivalent to their compromise. Therefore, in the image reconstruction process that migrates to other bone microstructures, the transition depends on deep networks and skip connections for SR reconstruction, lacking of migration and generalization capabilities. The Bicubic interpolation

method is equivalent to the degradation process of the image resolution preset, and lacks the applicability to different scenes.

It can also be found that the AESR model in this paper performs better on PSNR than the LapSRN method, which shows that the network combined with the auto-encoder structure has greater advantages in feature learning and expression. Moreover, with the decrease of the complexity of the test samples, other schemes have different degrees of fluctuation, and the performance of the AESR model is almost proportional to the complexity, and the gap with other models becomes more and more obvious. This shows that the proposed method can be applied to image content changes well based on the good feature expression ability of the auto-encoder structure itself, and has greater generalization and migration ability.

The curve change in Figure 2(b) below shows the comparison of the SSIM of the evaluation indicators of different models on the same data set.

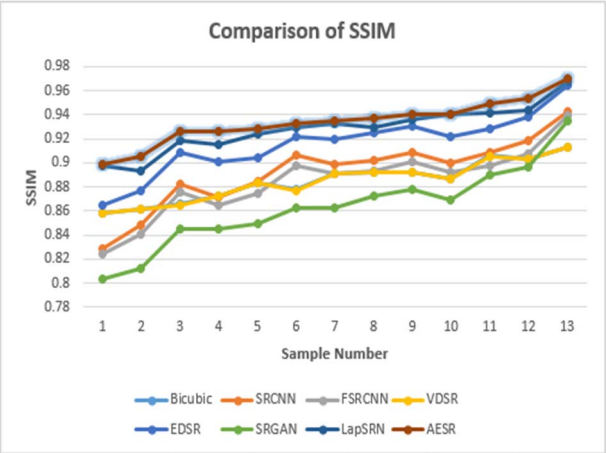

Figure 2(b) Comparison of the test results of each model on the evaluation index SSIM

For the trend change of SSIM, it is relatively compact. Even on the sample numbered 7, the LapSRN are almost the same as the method AESR mentioned in this paper. VDSR and Bicubic still have the same trend, and their performance is not satisfactory. This explains to a large extent that relying only on deepening the network level cannot meet the requirements of SR reconstruction, and cannot migrate applications well. Through observation, it can be found that, unlike the performance of PSNR, the curve changes of each model on SSIM are relatively stable, and the performance of the model increases with the decrease of image complexity. This indicates that SSIM index has a good performance in measuring the Micro-CT image of bone microstructure, the test sample used in this experiment. The structure on the Micro-CT image of the bone microstructure used in the experiment has a good measure of performance. This gives us the inspiration that in the application scenario focusing on image structure, we should pay more attention to SSIM evaluation indicators.

The superiority of the proposed method can be proved by the quantitative analysis of PSNR and SSIM. Moreover, in the method used for comparison verification, SRCNN, FSRCNN, EDSR and LapSRN also performed well, especially in the evaluation index SSIM, which is a good illustration of the validity of the data set constructed in this paper.

IV. Discussion

Figure 3 shows the test samples numbered 2, 9 and 13, and the comparison results. By observing Fig. 3(a), it can be found that the sample No.2 is very complicated, and all models perform poorly on it. Observing the curve changes of PSNR and SSIM, it can be found that all models fluctuate between Sample 6-10, but the overall maintenance is in a stable interval. As shown in Sample 9, the structure of such a sample is relatively loose and contains more noise, which may affect the weight change of the model in the feature extraction process, so that its performance slightly oscillates. Looking at Figure 3(c), it can be found that the bone microstructure of Sample 13 is complete and simple, and all models have achieved a high level of performance on SSIM. However, in the evaluation of PSNR, the AESR model mentioned in this paper has declined. The calculation of the PSNR index is closely related to the pixel value. Observing the real HR image and SR image of Sample 13 can be found that in the real HR image, most of the blank areas except the microstructure are full of noise, while on the SR image, it is a piece smooth. From the observation of Sample 13, these noises are not necessary for the reconstruction and application of the microstructure. Therefore, from this perspective, these models have a certain noise reduction effect on the HR image. Whether this noise reduction effect is beneficial, may be able to find certain evaluation indicators in the future work, or to screen according to the actual application effect, which will enable us to more comprehensively evaluate the reconstruction effect in the future research process, in order to facilitate practical application, development and promotion. For the benefit of removing sample data noise, this paper has made further exploration and verification.

A. Denoising

In the original data set (including training set and test set), the same method is used for noise reduction, a new training set and test set are obtained, and then the network model is used for training and testing again to compare with the previous results.

From the experimental results and comparative analysis in section III, we know that the proposed method surpasses other comparison models in both PSNR and SSIM evaluation indicators. Therefore, this part of the exploration verification only uses the model AESR proposed in this paper for training and testing.

In order to ensure the fairness of the comparative experiment, the training and test parameters on the new data set are consistent with the parameters of the experiment in III.

B. Results

First, observe the test results of the model before and

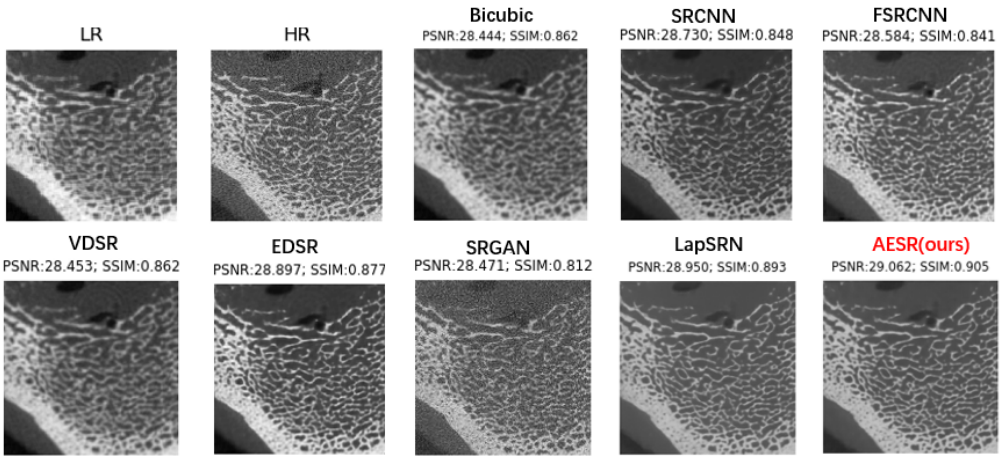

Figure 3(a) Test result of sample No. 2

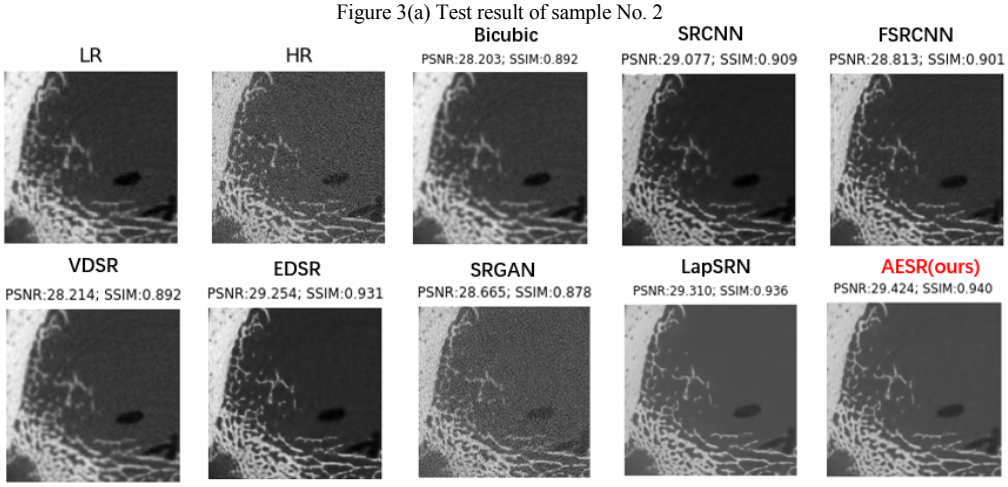

Figure 3(b) Test result for sample No. 9

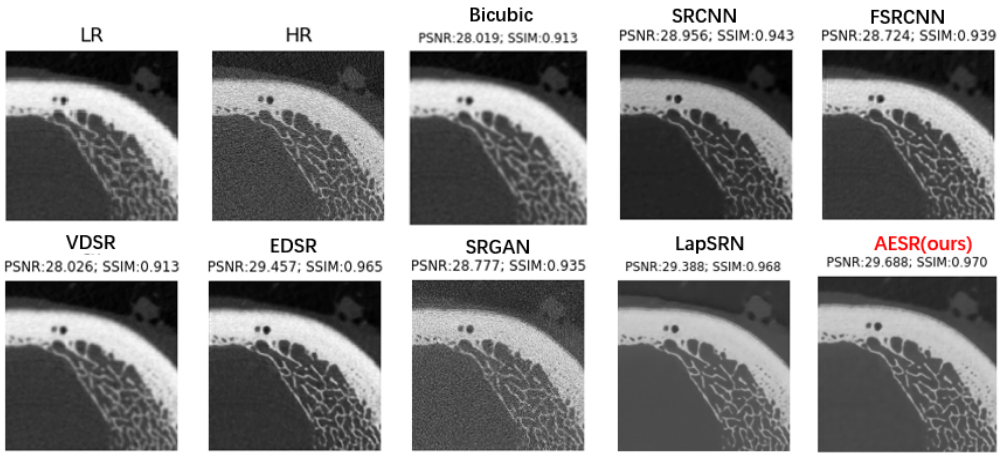

Figure 3(c) Test result of sample No. 13

after denoising for samples numbered 2, 9 and 13. As shown in Figure 4 below, it can be clearly seen that for the model AESR proposed in this paper, both the complex structure and the simple structure, the two evaluation indexes PSNR and SSIM after denoising are greatly improved. Moreover, from the perspective of visual perception, the reconstructed SR image has a stronger similarity with the real image HR. For the Bicubic method, the effect is not obvious, and there is a floating phenomenon (the PSNR index is decreased).

Figure 5 is a graph showing the change in the evaluation index of all samples before and after denoising. Comparing the curves in Figure 5, it is not difficult to find that both the Bicubic and AESR methods have a larger improvement effect on SSIM, and the AESR method is relatively larger. For the PSNR curve, the performance of Bicubic is mixed, while the AESR method has improved a lot. We analyzed that denoising smoothed the image, filtered out some noise, and had some effect on the PSNR based on pixel value calculation, and the result of this effect should be dependent on the denoising effect. For SSIM, based on contrast, brightness and structural similarity, smoothing reduces the negative effects of unrelated noise, and is more conducive to its focus on structural similarity calculations, so the improvement is more stable for both models.

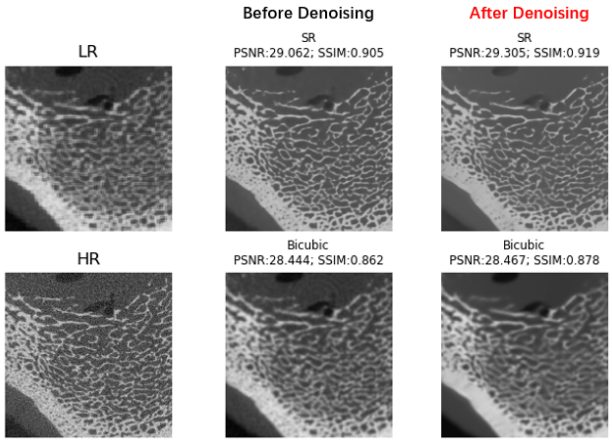

Figure 4 (a) Sample No.2 before and after denoising

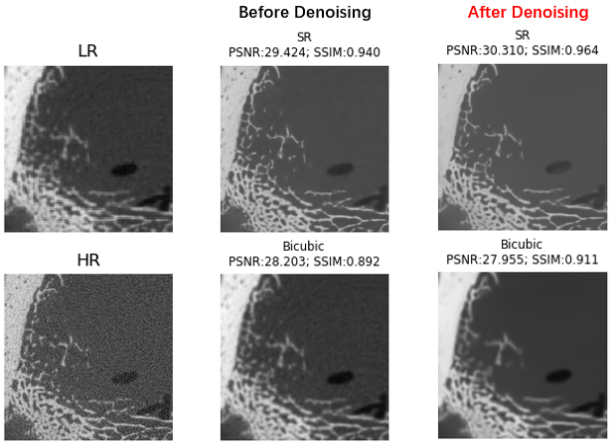

Figure 4 (b) Sample No.9 before and after denoising

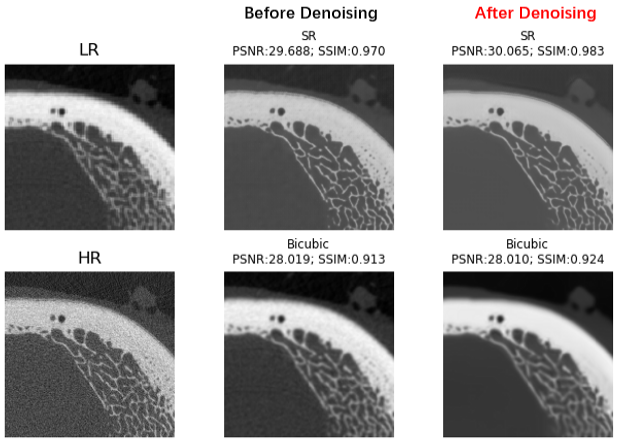

Figure 4 (c) Sample No.13 before and after denoising

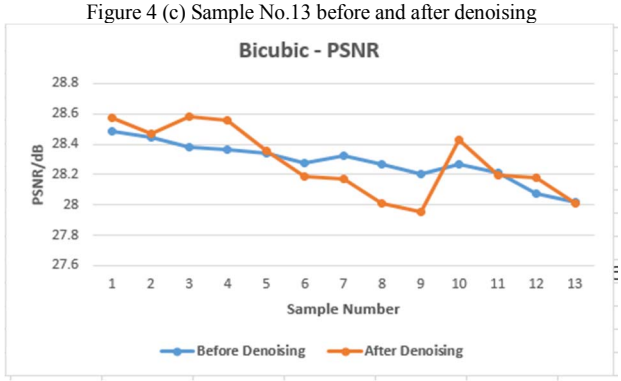

Figure 5(a) Changes in PSNR indicator using the Bicubic method before and after denoising

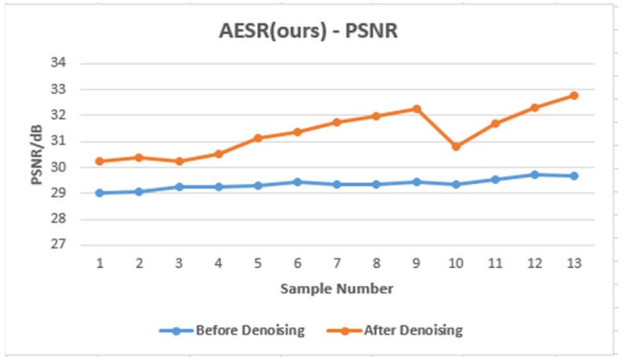

Figure 5(b) Changes in PSNR indicator using the AESR method before and after denoising

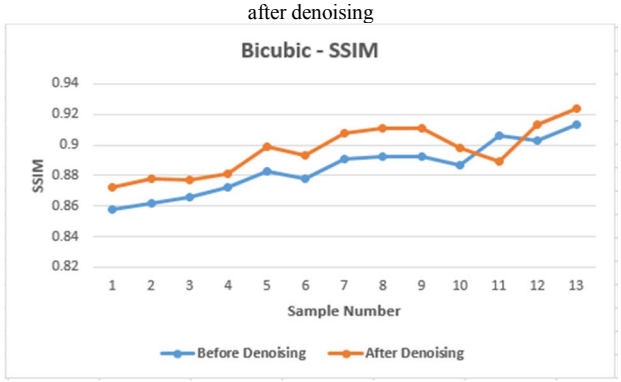

Figure 5(c) Changes in SSIM indicator using the Bicubic method before and after denoising

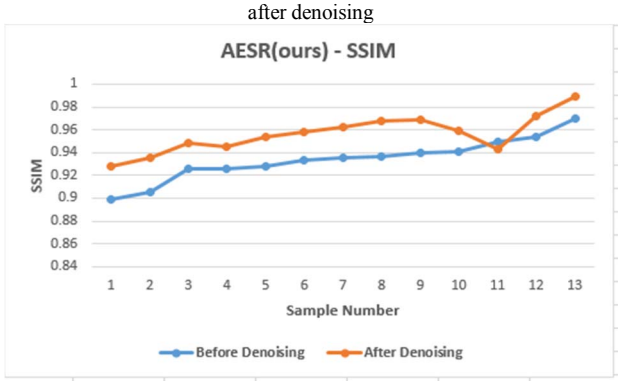

Figure 5(d) Changes in SSIM indicator using the AESR method before and after denoising

In summary, for the datasets used in this paper, the effects of noise reduction before and after noise reduction are compared using AESR and Bicubic methods. It is found that the noise reduction process has a great influence on the evaluation index, and its performance on SSIM is more stable and positive than PSNR. Therefore, for the bone microstructure data set constructed in this paper, the positive impact of noise reduction is greater than the negative impact. In future work, we may consider adding appropriate noise reduction measures and introducing new indicators to improve the evaluation of relevant research and applications.

V. Conclusion

For the super-resolution reconstruction of micro-CT images of bone microstructure, this paper firstly constructed a real LR-HR paired data set according to the needs of practical application scenarios, and verified its effectiveness by the existing model method. In the structural design of neural networks, this paper proposes a network model of auto-

encoder structure. Firstly, the high-resolution image output is constructed by means of staged up-sampling, and then the reconstructed image is down-sampled to the same resolution as the input LR using the learning method. The multi-stage weighted loss function is used to supervise and guide the network model autonomy excavate the characteristics of the image itself, and learn the mapping relationship between LR and HR, so as to reconstruct high-resolution images with rich details based on the learning of more effective information.

Combined with the quantitative and qualitative evaluation results, the quantitative calculation results of the proposed network structure on the test set are better than the traditional interpolation-based method and the deep learning-based method. Moreover, because the auto-encoder structure itself has good feature expression ability, the method proposed in this paper is not limited to CT image super-resolution reconstruction of bone microstructure, and has better applicability than other schemes.

Micro-CT images of bone microstructures have spatial continuity. Although the method described in this paper has achieved good performance, in the process of constructing data sets and training, the spatial correlation between images is neglected, and only the reconstruction process of single images is considered. Therefore, in the next study, we consider using 3D neural networks to further improve the super-resolution reconstruction of medical CT images. Moreover, for the evaluation index of the reconstruction effect, it is proposed to consider adding statistical information such as the covariance matrix [24] to further conform to the actual operational requirements. For practical clinical applications, considering the difference in imaging conditions between clinical CT and Micro-CT images, it is also necessary to consider the problem of image registration [25], which needs further exploration.

REFERENCES

[1] Kleerekoper, Michael, et al. "The role of three-dimensional trabecular microstructure in the pathogenesis of vertebral compression fractures." Calcified Tissue International 37.6 (1985): 594-597.

[2] Legrand, Erick, et al. "Trabecular Bone Microarchitecture, Bone Mineral Density, and Vertebral Fractures in Male Osteoporosis." Journal of Bone and Mineral Research 15.1 (2000): 13-19.

[3] Parfitt, A. M., et al. "Relationships between surface, volume, and thickness of iliac trabecular bone in aging and in osteoporosis. Implications for the microanatomic and cellular mechanisms of bone loss." Journal of Clinical Investigation 72.4 (1983): 1396-1409.

[4] Ding, Ming, and Ivan Hvid. "Quantification of age-related changes in the structure model type and trabecular thickness of human tibial cancellous bone." Bone 26.3 (2000): 291-295.

[5] Purkait, Pulak, and Bhabatosh Chanda. "Super Resolution Image Reconstruction Through Bregman Iteration Using Morphologic Regularization." IEEE Transactions on Image Processing 21.9 (2012): 4029-4039.

[6] Yang, Jianchao, et al. "Image Super-Resolution Via Sparse Representation." IEEE Transactions on Image Processing 19.11 (2010): 2861-2873.

[7] Dong, Chao, et al. "Image Super-Resolution Using Deep Convolutional Networks." IEEE Transactions on Pattern Analysis and Machine Intelligence 38.2 (2016): 295-307.

[8] Dong, Chao, et al. "Learning a Deep Convolutional Network for Image Super-Resolution." european conference on computer vision (2014): 184-199.

[9] You, Chenyu, et al. "CT Super-resolution GAN Constrained by the Identical, Residual, and Cycle Learning Ensemble(GAN-CIRCLE)." arXiv: Image and Video Processing (2018).

[10] Uzunova, Hristina, et al. "Multi-scale GANs for Memory-efficient Generation of High Resolution Medical Images.." arXiv: Image and Video Processing (2019).

[11] Chaudhari, Akshay S., et al. "Super‐resolution musculoskeletal MRI using deep learning." Magnetic Resonance in Medicine 80.5 (2018): 2139-2154.

[12] H. Yu, D. Liu, H. Shi, H. Yu, Z. Wang, X. Wang, B. Cross, M. Bramler, and T. S. Huang, "Computed tomography super-resolution using convolutional neural networks," in Proc. IEEE Intl. Conf. Image Process., 2017, pp. 3944–3948.

[13] Liu, Jia, et al. "An Edge Enhanced SRGAN for MRI Super Resolution in Slice-Selection Direction." Multimodal Brain Image Analysis and Mathematical Foundations of Computational Anatomy. Springer, Cham, 2019. 12-20.

[14] Lai, Wei-Sheng, et al. "Deep laplacian pyramid networks for fast and accurate super-resolution." Proceedings of the IEEE conference on computer vision and pattern recognition. 2017.

[15] Liu, Pan, Chao Li, and Carola-Bibiane Schönlieb. "GANReDL: Medical Image Enhancement Using a Generative Adversarial Network with Real-Order Derivative Induced Loss Functions." International Conference on Medical Image Computing and Computer-Assisted Intervention. Springer, Cham, 2019.

[16] Xuan, Kai, et al. "Reconstruction of Isotropic High-Resolution MR Image from Multiple Anisotropic Scans Using Sparse Fidelity Loss and Adversarial Regularization." International Conference on Medical Image Computing and Computer-Assisted Intervention. Springer, Cham, 2019.

[17] Chen, Yuhua, et al. "Efficient and accurate MRI super-resolution using a generative adversarial network and 3D multi-level densely connected network." International Conference on Medical Image Computing and Computer-Assisted Intervention. Springer, Cham, 2018.

[18] Gu, Jinjin, et al. "Blind super-resolution with iterative kernel correction." Proceedings of the IEEE Conference on Computer Vision and Pattern Recognition. 2019.

[19] Shi, Wenzhe, et al. "Real-time single image and video super-resolution using an efficient sub-pixel convolutional neural network." Proceedings of the IEEE conference on computer vision and pattern recognition. 2016.

[20] Dong, Chao, Chen Change Loy, and Xiaoou Tang. "Accelerating the super-resolution convolutional neural network." European conference on computer vision. Springer, Cham, 2016.

[21] Kim, Jiwon, Jung Kwon Lee, and Kyoung Mu Lee. "Accurate image super-resolution using very deep convolutional networks." Proceedings of the IEEE conference on computer vision and pattern recognition. 2016.

[22] Lim, Bee, et al. "Enhanced Deep Residual Networks for Single Image Super-Resolution." arXiv: Computer Vision and Pattern Recognition (2017).

[23] Ledig, Christian, et al. "Photo-realistic single image super-resolution using a generative adversarial network." Proceedings of the IEEE conference on computer vision and pattern recognition. 2017.

[24] Zhe Min et al. "Statistical Model of Total Target Registration Error In Image-Guided Surgery", TASE 2019.

[25] Zhe Min, et al "Generalized Non-rigid point set registration with hybrid mixture models considering anisotropic positional uncertainties", MICCAI 2019.